ARTICLES
https://doi.org/10.1038/s41567-020-0877-x

nature physics

Room-temperature optomechanical squeezing

Nancy Aggarwal[1,4]✉, Torrey J. Cullen[2], Jonathan Cripe[2], Garrett D. Cole[3,5], Robert Lanza[1], Adam Libson[1], David Follman[3,5], Paula Heu[3], Thomas Corbitt[2]✉ and Nergis Mavalvala[1]✉

Squeezed light—light with quantum noise lower than shot noise in some quadratures and higher in others—can be used to improve the sensitivity of precision measurements. In particular, squeezed light sources based on nonlinear optical crystals are being used to improve the sensitivity of gravitational wave detectors. In optomechanical squeezers, the radiation-pressure-driven interaction of a coherent light field with a mechanical oscillator induces correlations between the amplitude and phase quadratures of the light, which induce the squeezing. However, thermally driven fluctuations of the mechanical oscillator's position make it difficult to observe the quantum correlations at room temperature and at low frequencies. Here, we present a measurement of optomechanically squeezed light, performed at room temperature in a broad band near the audio-frequency regions relevant to gravitational wave detectors. We observe sub-Poissonian quantum noise in a frequency band of 30–70 kHz with a maximum reduction of 0.7 ± 0.1 dB below shot noise at 45 kHz. We present two independent methods of measuring this squeezing, one of which does not rely on the calibration of shot noise.

Measurements whose sensitivity is limited by quantum noise can be improved by modifying the distribution of quantum noise. For example, the shot noise limit of optical measurements using coherent states of light can be improved by using squeezed states[1–3]. Squeezing methods employ light with uncertainty below shot noise in the signal quadrature at the expense of increased noise in orthogonal quadratures. As a result of this redistribution of uncertainty, squeezed states can enhance the precision of measurements that are otherwise limited by quantum noise. The preeminent example is interferometric gravitational wave (GW) detectors, where squeezed state injection lowers the noise floor below shot noise[1,2,4–6].

Squeezed states of light suitable for GW detectors have been successfully generated using nonlinear optical materials[5–9]. Similarly, the optomechanical (OM) interaction is an effective nonlinearity[10] for the light field, which can squeeze its quantum fluctuations[4,11–14]. OM squeezing has some advantages over squeezed state generation using nonlinear optical media. It can be generated independently of the optical wavelength, with a tunable frequency dependence of the squeezing quadrature via the optical spring (ref. [14] and N. Aggarwal et al., in preparation), and in the long term, OM squeezers have great potential to be miniaturized.

Previously, OM squeezing has been observed[15–20] in systems operated close to the mechanical resonance (within an octave). Although these experiments laid important foundations for OM squeezed light, some important challenges for practical OM squeezed light sources have remained. For GW detection, for example, the squeezed light source needs to be broadband over three decades in the audio-frequency band, compact and operate stably, 24/7, at room temperature. Here, we present a measurement of squeezing produced by an OM system that is composed of a Fabry–Pérot interferometer with a microscale mirror as a mechanical oscillator at room temperature, where OM squeezing has been observed in a room-temperature system at frequencies as low as tens of kilohertz and extending more than a decade away from the mechanical resonance. This observation of broadband OM squeezing at room temperature presents a new avenue for building quantum OM resources at room temperature that are independent of laser wavelength.

Overcoming thermal noise[21] has been a fundamental challenge in the observation of optomechanically generated squeezing beyond cryogenic temperatures. Reducing the quantum noise below shot noise in such a system is only possible if the motion of the oscillator has a significant contribution from quantum radiation pressure noise (QRPN) and is not overwhelmed by thermal fluctuations (N. Aggarwal et al., in preparation; S. Sharifi et al., in preparation). Our mechanical oscillators are designed to have extremely low broadband thermal noise (refs. [22–25] and S. Sharifi et al., in preparation) and have been used to observe QRPN[26]. The thermal noise of these oscillators is sufficiently low to not overwhelm the effect of QRPN. Even so, thermal noise does limit the amount of measurable squeezing generated. In addition to the limitation set by thermal noise, our locking and detection scheme introduces losses that degrade some of the quantum correlations created by the OM coupling. Thermal noise, lossy detection and cavity-feedback noise together limit the amount of squeezing and the frequency band in which it is observed.

A precise calibration of shot noise has been the basis for all prior demonstrations of OM squeezing. We demonstrate a technique based on photocurrent correlations that obviates the need for such a calibration. This technique may be useful on its own for future studies of squeezing in general.

Our experimental set-up consists of two main subsystems—the OM cavity and the detection system (Fig. 1). The OM system is a Fabry–Pérot cavity, housed in a vacuum chamber (~10^{-7} torr) and pumped with a 1,064-nm Nd:YAG non-planar ring oscillator (NPRO) laser. One of the two mirrors of this cavity is supported by a low-noise single-crystal microcantilever (similar to that employed in ref. [26]), with a mass of 50 ng, a fundamental frequency of 876 Hz and a mechanical quality factor of 16,000. The other mirror is a 0.5-in-diameter mirror with a radius of curvature of 1 cm. The cavity is just under 1 cm long and has a finesse of ~11,500 and a half-width at half-maximum (HWHM) linewidth (γ) of 650 kHz.

We lock the cavity blue-detuned about 0.33γ away from resonance, using the strong optical spring (145 kHz) created by the detuned operation[14]. This high optical rigidity, with a spring constant of ~41 N m^{-1}, can be put into perspective by converting it into

[1]LIGO – Massachusetts Institute of Technology, Cambridge, MA, USA. [2]Department of Physics, Louisiana State University, Baton Rouge, LA, USA. [3]Crystalline Mirror Solutions, Santa Barbara, CA, USA. [4]Present address: Northwestern University, Evanston, IL, USA. [5]Present address: Thorlabs Crystalline Solutions, Santa Barbara, CA, USA. ✉e-mail: nancyagg@mit.edu; tcorbitt@phys.lsu.edu; nergis@mit.edu

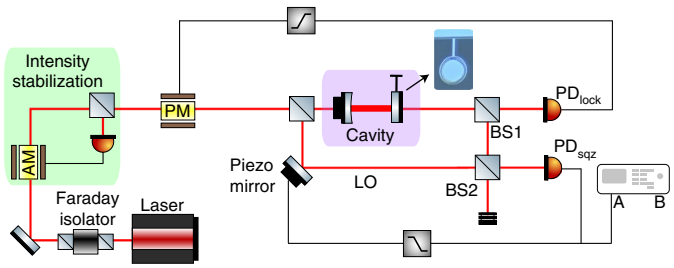

Fig. 1 | An overview of the main subsystems in the experiment. The classical intensity noise of a 1,064-nm Nd:YAG laser is suppressed by an intensity stabilization servo using an amplitude modulator (AM) as the actuator. The light is then sent to an OM cavity, where the input mirror is a mechanically rigid macromirror and the output mirror is a low-noise microscale mirror supported by a single-crystal microcantilever. The light inside this cavity is squeezed due to the radiation pressure interaction between the circulating light and the movable micromirror. The cavity is locked by picking off 15% of the transmitted power through beamsplitter BS1 on photodetector PD_{lock}, and feeding back that signal to a phase modulator (PM). The remaining 85% of the light is interfered with a local oscillator (LO) on BS2, which reflects 96.5% of the light and transmits 3.5%. The phase between the LO and the signal is locked by feeding back the d.c. part of the fringe detected on PD_{sqz} to a piezo mirror in the LO path. The signal from PD_{sqz} is also sent into the spectrum analyser for measurement.

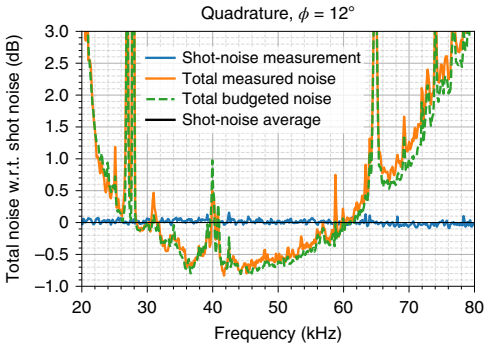

Fig. 2 | Measured spectrum and modelled noise budget at 12° quadrature. All quadrature angles are referenced so that 0° corresponds to the amplitude quadrature of the cavity transmission. This figure shows the measured spectrum relative to shot noise. We show the shot-noise measurement in blue, which is used to obtain an average shot-noise level. All data in this paper are scaled to this average shot-noise level. The spectrum for total measured noise at 12° is shown in orange, showing squeezing from 30 kHz to 60 kHz, with maximum squeezing of 0.7 ± 0.1 dB (corresponding to a 15 ± 2% reduction in PSD) near 45 kHz. We also show the total budgeted noise as a dashed green line; this is a quadrature sum of quantum noise, thermal noise, classical laser noise, cavity-feedback noise and differential phase noise.

an effective Young's modulus of a bar of the size of the optical beam[27]. For a cavity of length 1 cm and an optical beam size of 100 µm, the equivalent Young's modulus is ~13 MPa. The high optical rigidity gives a flat spectrum below the OM resonant frequency, allowing for frequency-independent squeezing up to hundreds of kilohertz while keeping a low thermal noise. To compare, if we required the same level of thermal noise from a mechanical oscillator with a natural frequency of 145 kHz, the required mechanical quality factor would be $16{,}000 \times (145{,}000/876)^2 = 4.4 \times 10^8$. Our relatively low mechanical quality factor allows for the same performance because of the optical dilution of the mechanical dissipation[28]. The optical spring has a strong suppression due to its rigidity, but is unstable, so electronic feedback at frequencies near the optical spring is used to stabilize the system using the transmitted light for the error signal. We use radiation pressure as the actuator for locking, as detailed in ref. [29], with one difference: in this experiment, we use a phase modulator (PM) as our actuator instead of an amplitude modulator. We can treat the instability of the optical spring in the same way, except for a slightly modified plant transfer function (N. Aggarwal and N. Mavalvala, in preparation). The open-loop gain of the cavity-locking loop is below one at all frequencies less than 140 kHz. Because we must obtain a signal to stabilize the optical spring while leaving the squeezed light available to be measured independently, we split the light exiting the cavity at a beamsplitter (BS1), using 15% of the total light to obtain the feedback error signal. This method introduces some common phase noise between the LO and the cavity field, which is included in our noise budget.

Traditionally, balanced homodyne detection is used to characterize squeezing, because it cancels classical intensity noise of the LO and does not introduce loss. In our set-up, however, we use a different method to measure the squeezing. This is because the classical intensity noise is sufficiently small to not require cancellation, and the level of squeezing we expect is low, making it insensitive to a small loss. The beam transmitted from the cavity (signal) is combined with a LO beam on a 96.5–3.5% beamsplitter (BS2), as shown in Fig. 1. We then measure the port that has 96.5% signal and 3.5% LO on a photodetector (PD_{sqz}). The output of PD_{sqz} is low-pass-filtered, amplified and then fed back to a piezoelectric crystal driving the length of the LO path. This loop suppresses relative path length fluctuations between the signal and the LO, but only at frequencies well below the measurement band. The loop has a unity gain frequency of less than 1 kHz and has an open-loop gain of less than −40 dB at the measurement frequencies, as shown in Extended Data Fig. 6. This eliminates the need to correct the squeezing spectrum for the response of the feedback loop. Additionally, there is no crossover between the homodyne loop and the cavity loop because their frequency regions of actuation are disjoint. Note that, because PD_{sqz} is an out-of-loop detector for both the cavity-locking as well as the homodyne-locking loop, a sub-shot-noise measurement on it is an indication of squeezing[30]. The lock maintains PD_{sqz} at a constant d.c. voltage level, which we use to calibrate the shot-noise level. The measurement quadrature is determined by the relative path length between the signal and LO. In the laboratory, the measurement quadrature can be tuned by changing either the lockpoint level, the LO power or both (see equations (11–14) in the Methods and Extended Data Fig. 5).

To compare the measured noise to shot noise, we measure the shot-noise level by turning off the homodyne lock, blocking the signal port and tuning the LO power to get the same voltage on PD_{sqz} as our lockpoint. This allows us to measure a spectrum of PD_{sqz} that contains the shot noise of the light, classical intensity noise and the dark noise of PD_{sqz}. We then average this spectrum over our measurement band to obtain the reference level (0 dB). Classical relative intensity noise (RIN) is suppressed by an intensity stabilization servo (ISS) to $\sim 8 \times 10^{-9}\,\mathrm{Hz}^{-1/2}$ and contributes less than −20 dB of the noise on PD_{sqz} (Extended Data Fig. 4). The RIN level is independently measured by performing a correlation measurement between PD_{sqz} and another pick-off between the ISS and the PM. Dark noise accounts for ~−12 dB of the shot-noise level (Extended Data Fig. 4) and is not subtracted.

The result of the homodyne measurement of the signal is shown in Fig. 2[31]. For a quadrature angle of 12 ± 2° from the amplitude quadrature, we observe up to 0.7 ± 0.1 dB of squeezing (equivalent to a 15 ± 2% reduction in the power spectral density (PSD)), from 30 kHz to 60 kHz.

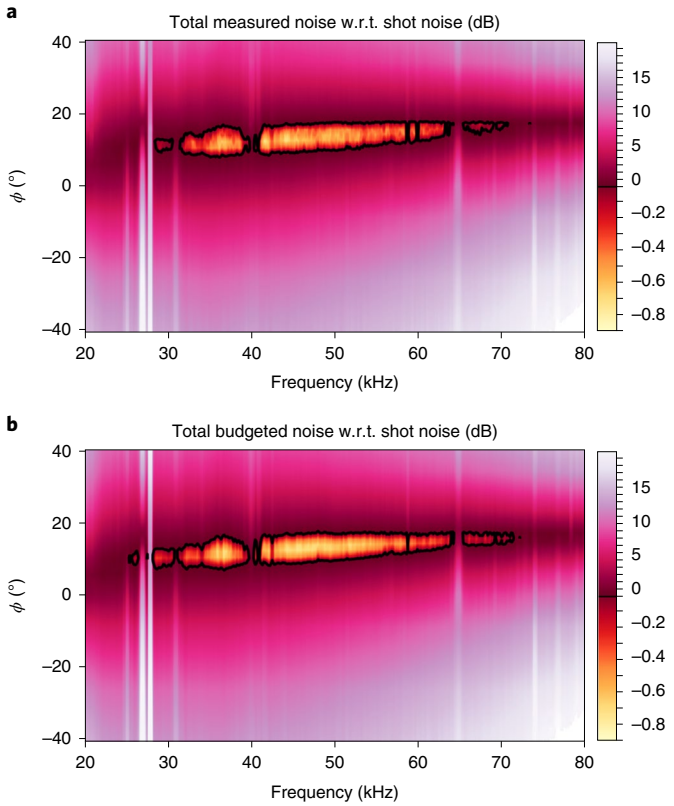

Fig. 3 | Measured and budgeted noises on PD_{sqz} at 14 different quadratures, distributed more densely near the squeezing quadrature and sparsely elsewhere. a, Measured noise relative to shot noise. **b**, Budgeted noise relative to shot noise. In both panels, black contour lines correspond to shot noise; the regions inside them are squeezed (shown by yellow-orange shades) and the regions outside are antisqueezed (shown by the upper pink shades). Squeezing is observed from 10° to 17° and from 30 kHz to 70 kHz. One of the mechanical modes of the cantilever can be seen at 27 kHz. As is characteristic of OM squeezing below the optical spring frequency (N. Aggarwal et al., in preparation), the higher quadrature shot-noise crossing for all frequencies occurs at the same quadrature. The upper part of the shot-noise contour is nearly perfectly horizontal.

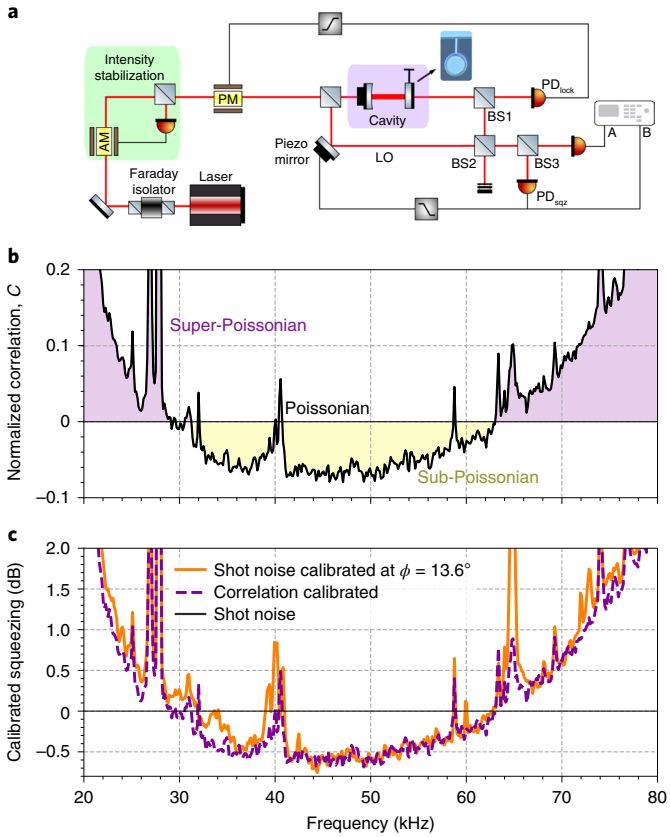

Fig. 4 | Calibration of squeezing by using correlations instead of measuring shot noise. a, Set-up for correlation measurement. We set the LO such that the field after BS2 is amplitude-squeezed and pass it through a 50–50 beamsplitter (BS3). We then perform a cross-spectrum measurement of the two outputs and normalize it to the individual spectra. This quantity can only be negative if the input beam is squeezed in the amplitude quadrature (see equation (3) in the Methods). **b**, Measurement of negative correlations. The existence of these negative correlations provides a verification of squeezing and allows for a shot-noise-independent way of verifying the existence of amplitude squeezing. **c**, The purple dashed curve shows the squeezing spectrum calibrated by using the negative correlations, without measuring shot noise (see equation (7) in the Methods). The orange solid line shows the spectrum calibrated by separately measuring the shot noise.

The distribution of squeezing is studied in detail by measurements of other quadratures of the homodyne signal. To do this without changing the locking loop or shot noise, we keep the homodyne locking offset the same, and vary the LO power. This allows us to change the measurement quadrature in a shot-noise-invariant way. In Fig. 3a, we show this measurement as a function of sideband frequency and quadrature.

To understand the observed squeezing, a detailed noise budget of the system is developed. The total budgeted noise in the squeezing quadrature is shown in Fig. 2, and in a quadrature-dependent way in Fig. 3b. This noise budget includes a model[32] that predicts the contribution of quantum noise and previously measured thermal noise[33] for the measured cavity and homodyne parameters as well as measured cavity-feedback injected noise and differential phase noise between the LO and the cavity. Finally, the extra loss in the detection path is obtained by comparing the measurement and noise budget at all frequencies and quadratures. Further details on the noise budget are provided in the Methods and Extended Data Figs. 2 and 3. As we see, the overall behaviour of the system is similar in the measurement as well as noise budget, most importantly the squeezing quadrature. The detailed noise budget can be used to infer the squeezing performance achievable by this particular device in the absence of technical noise and excess loss, as shown in Extended Data Fig. 1.

For additional evidence of squeezing, we also performed a correlation measurement on the squeezed light. Extending the approaches in refs. [34–38], we demonstrate that these correlations are a way to characterize a squeezed light source without measuring shot noise. The light exiting the cavity, after combination with the LO, is split equally between two photodetectors, as shown in Fig. 4a. As described in the Methods, if the light is limited by classical noise, positive correlations should be observed in the two photocurrents. Shot-noise-limited light should produce zero correlations, and intensity-squeezed light should produce negative correlations. We measured the cross-power spectrum between the two photodetectors and confirmed that negative correlations are observed, as shown in Fig. 4b. The cross-spectrum is negative from 33 kHz to 62 kHz and positive elsewhere, which agrees with the measured spectrum in Fig. 2. For explicit comparison, we converted this correlation to the squeezing factor (using equation (7) in the Methods). This squeezing factor is shown in Fig. 4c as a dashed purple line.

This provides unconditional evidence that the light is squeezed at these frequencies and at this quadrature. In the same plot, we also show the squeezing spectrum obtained using the traditional way of measuring shot noise separately (solid orange line). This orange curve corresponds to a shot-noise-calibrated measurement at 13.6°. This spectrum is obtained by interpolating the shot-noise-calibrated measurements over various quadratures and using the interpolated dataset to minimize the residual between the correlation-calibrated measurement and the shot-noise-calibrated measurement. The quadrature that minimizes this residual is $\phi = 13.6°$. This would be possible if the correlation measurement were made at a slightly different quadrature as compared to the shot-noise-calibrated measurement. The difference between the quadratures can be attributed to the error in inference of quadrature due to uncertainty in the measurement of optical power. Once this error in measurement quadrature between the two methods is accounted for, the two methods are in excellent agreement with each other.

This system, as a squeezed-light source for GW measurements or as a source of other quantum states like entangled states, makes a wavelength-agnostic, miniature, robust quantum resource at room temperature. In addition to OM squeezing and exploring broadband quantum correlations at room temperature, this system also opens up a broad range of possibilities for quantum measurements on multimode OM systems that exhibit quantum-mechanical behaviour in a thermal bath[39–42], as well as quantum-mechanically calibrated temperature[43,44] measurements. More generally, it brings us one step closer to experimentally investigating the interplay of quantum systems with classical decoherence mechanisms like thermal fluctuations and gravitational forces[45–52].

Online content

Any methods, additional references, Nature Research reporting summaries, source data, extended data, supplementary information, acknowledgements, peer review information; details of author contributions and competing interests; and statements of data and code availability are available at https://doi.org/10.1038/s41567-020-0877-x.

Received: 28 May 2019; Accepted: 12 March 2020;
Published online: 7 July 2020

References

1. Caves, C. M. Quantum-mechanical noise in an interferometer. *Phys. Rev. D* **23**, 1693–1708 (1981).
2. Caves, C. M. Quantum-mechanical radiation-pressure fluctuations in an interferometer. *Phys. Rev. Lett.* **45**, 75–79 (1980).
3. Gerry, C., Knight, P. & Knight, P. L. *Introductory Quantum Optics* (Cambridge Univ. Press, 2005).
4. Kimble, H. J., Levin, Y., Matsko, A. B., Thorne, K. S. & Vyatchanin, S. P. Conversion of conventional gravitational-wave interferometers into quantum nondemolition interferometers by modifying their input and/or output optics. *Phys. Rev. D* **65**, 022002 (2001).
5. LIGO Scientific Collaboration et al. Enhanced sensitivity of the LIGO gravitational wave detector by using squeezed states of light. *Nat. Photon.* **7**, 613–619 (2013).
6. Grote, H. et al. First long-term application of squeezed states of light in a gravitational-wave observatory. *Phys. Rev. Lett.* **110**, 181101 (2013).
7. Wu, L.-A., Kimble, H. J., Hall, J. L. & Wu, H. Generation of squeezed states by parametric down conversion. *Phys. Rev. Lett.* **57**, 2520–2523 (1987).
8. Schnabel, R., Mavalvala, N., McClelland, D. E. & Lam, P. K. Quantum metrology for gravitational wave astronomy. *Nat. Commun.* **1**, 121 (2010).
9. Schnabel, R. Squeezed states of light and their applications in laser interferometers. *Phys. Rep.* **684**, 1–51 (2017).
10. Aspelmeyer, M., Kippenberg, T. J. & Marquardt, F. Cavity optomechanics. *Rev. Mod. Phys.* **86**, 1391–1452 (2014).
11. Mancini, S. & Tombesi, P. Quantum noise reduction by radiation pressure. *Phys. Rev. A* **49**, 4055–4065 (1994).
12. Fabre, C. et al. Quantum-noise reduction using a cavity with a movable mirror. *Phys. Rev. A* **49**, 1337–1343 (1994).
13. Harms, J. et al. Squeezed-input, optical-spring, signal-recycled gravitational-wave detectors. *Phys. Rev. D* **68**, 042001 (2003).
14. Corbitt, T. et al. Squeezed-state source using radiation-pressure-induced rigidity. *Phys. Rev. A* **73**, 023801 (2006).
15. Brooks, D. W. C. et al. Non-classical light generated by quantum-noise-driven cavity optomechanics. *Nature* **488**, 476–480 (2012).
16. Safavi-Naeini, A. H. et al. Squeezed light from a silicon micromechanical resonator. *Nature* **500**, 185–189 (2013).
17. Purdy, T. P., Yu, P.-L. L., Peterson, R. W., Kampel, N. S. & Regal, C. A. Strong optomechanical squeezing of light. *Phys. Rev. X* **3**, 031012 (2013).
18. Sudhir, V. et al. Appearance and disappearance of quantum correlations in measurement-based feedback control of a mechanical oscillator. *Phys. Rev. X* **7**, 011001 (2017).
19. Ockeloen-Korppi, C. F., Damskägg, E., Paraoanu, G. S., Massel, F. & Sillanpää, M. A. Revealing hidden quantum correlations in an electromechanical measurement. *Phys. Rev. Lett.* **121**, 243601 (2018).
20. Barzanjeh, S. et al. Stationary entangled radiation from micromechanical motion. *Nature* **570**, 480–483 (2019).
21. Saulson, P. R. Thermal noise in mechanical experiments. *Phys. Rev. D* **42**, 2437–2445 (1990).
22. Cole, G. D., Gröblacher, S., Gugler, K., Gigan, S. & Aspelmeyer, M. Monocrystalline $Al_xGa_{1-x}As$ heterostructures for high-reflectivity high-Q micromechanical resonators in the megahertz regime. *Appl. Phys. Lett.* **92**, 261108 (2008).
23. Cole, G. D. Cavity optomechanics with low-noise crystalline mirrors. In *Proceedings of SPIE 8458*, *Optics*, *Photonics*, *Optical Trapping and Optical Micromanipulation IX* 845807 (SPIE, 2012).
24. Cole, G. D. et al. High-performance near- and mid-infrared crystalline coatings. *Optica* **3**, 647–656 (2016).
25. Singh, R., Cole, G. D., Cripe, J. & Corbitt, T. Stable optical trap from a single optical field utilizing birefringence. *Phys. Rev. Lett.* **117**, 213604 (2016).
26. Cripe, J. et al. Measurement of quantum back action in the audio band at room temperature. *Nature* **568**, 364–367 (2019).
27. Corbitt, T. et al. An all-optical trap for a gram-scale mirror. *Phys. Rev. Lett.* **98**, 150802 (2007).
28. Corbitt, T. et al. Optical dilution and feedback cooling of a gram-scale oscillator to 6.9 mK. *Phys. Rev. Lett.* **99**, 160801 (2007).
29. Cripe, J. et al. Radiation-pressure-mediated control of an optomechanical cavity. *Phys. Rev. A* **97**, 013827 (2018).
30. Wiseman, H. M. Squashed states of light: theory and applications to quantum spectroscopy. *J. Opt. B* **1**, 459 (1999).
31. Aggarwal, N. Data and analysis behind the publication 'Room temperature optomechanical squeezing' (Zenodo, 2020); https://zenodo.org/record/3694290
32. Corbitt, T., Chen, Y. & Mavalvala, N. Mathematical framework for simulation of quantum fields in complex interferometers using the two-photon formalism. *Phys. Rev. A* **72**, 013818 (2005).
33. Cripe, J. et al. Quantum back action cancellation in the audio band. Preprint at https://arxiv.org/pdf/1812.10028.pdf (2018).
34. Bartley, T. J. et al. Direct observation of sub-binomial light. *Phys. Rev. Lett.* **110**, 173602 (2013).
35. Kimble, H. J., Dagenais, M. & Mandel, L. Photon antibunching in resonance fluorescence. *Phys. Rev. Lett.* **39**, 691–695 (1977).
36. McCuller, L. *Effect of Squeezing on the OMC DCPD Cross Correlation* LIGO-T1800110-v1 (2018); https://dcc.ligo.org
37. Krivitsky, L. A. et al. Correlation measurement of squeezed light. *Phys. Rev. A* **79**, 033828 (2009).
38. Heidmann, A. et al. Observation of quantum noise reduction on twin laser beams. *Phys. Rev. Lett.* **59**, 2555–2557 (1987).
39. Nielsen, W. H. P., Tsaturyan, Y., Møller, C. B., Polzik, E. S. & Schliesser, A. Multimode optomechanical system in the quantum regime. *Proc. Natl Acad. Sci. USA* **114**, 62–66 (2017).
40. Hsiang, J.-T. & Hu, B.-L. Quantum thermodynamics at strong coupling: operator thermodynamic functions and relations. *Entropy* **20**, 423 (2018).
41. Hakim, V. & Ambegaokar, V. Quantum theory of a free particle interacting with a linearly dissipative environment. *Phys. Rev. A* **32**, 423–434 (1985).
42. de Lépinay, L. M., Pigeau, B., Besga, B. & Arcizet, O. Eigenmode orthogonality breaking and anomalous dynamics in multimode nano-optomechanical systems under non-reciprocal coupling. *Nat. Commun.* **9**, 1401 (2018).
43. Purdy, T. P. et al. Optomechanical Raman-ratio thermometry. *Phys. Rev. A* **92**, 031802 (2015).
44. Purdy, T. P., Grutter, K. E., Srinivasan, K. & Taylor, J. M. Quantum correlations from a room-temperature optomechanical cavity. *Science* **356**, 1265–1268 (2017).
45. Spohn, H. & Lebowitz, J. L. *Irreversible Thermodynamics for Quantum Systems Weakly Coupled to Thermal Reservoirs* 109–142 (Wiley, 2007).
46. Smith, A. et al. Verification of the quantum nonequilibrium work relation in the presence of decoherence. *New J. Phys.* **20**, 013008 (2018).
47. Ashida, Y., Saito, K. & Ueda, M. Thermalization and heating dynamics in open generic many-body systems. *Phys. Rev. Lett.* **121**, 170402 (2018).
48. Milburn, G. J. Decoherence and the conditions for the classical control of quantum systems. *Philos. Trans. R. Soc. A* **370**, 4469–4486 (2012).

49. Kafri, D., Taylor, J. M. & Milburn, G. J. A classical channel model for gravitational decoherence. *New J. Phys.* **16**, 065020 (2014).
50. Diósi, L. Gravitation and quantum-mechanical localization of macro-objects. *Phys. Lett. A* **105**, 199–202 (1984).
51. Penrose, R. On gravity's role in quantum state reduction. *Gen. Relat. Gravit.* **28**, 581–600 (1996).
52. Marshall, W., Simon, C., Penrose, R. & Bouwmeester, D. Towards quantum superpositions of a mirror. *Phys. Rev. Lett.* **91**, 130401 (2003).

Methods

Application to precision measurements. In addition to being wavelength-agnostic and compact, an OM squeezer innately generates a bright squeezed field. This means an OM squeezed field comes with its own internal phase reference, hence eliminating the need for an extra coherent phase-locking field[5,53]. For example, if the state after BS2 in Fig. 1 were sent to a precision measurement set-up, it would include the carrier field, which provides a self-referenced signal to allow locking to the correct squeezing quadrature. In contrast, vacuum squeezed states generated by a nonlinear crystal have to be accompanied by an extra and usually frequency-shifted optical beam that keeps track of the squeezing quadrature[5,53].

Although the current level of squeezing in our set-up is limited by extraneous technical noises, in the absence of those noises, the squeezing would be limited by intracavity losses. This expected squeezing in the absence of extraneous noise is shown in Extended Data Fig. 1. After elimination of differential phase noise between the LO and cavity, the squeezing would extend to much lower frequencies. The differential phase noise injected into the system can be reduced by picking off and recombining the LO inside the vacuum where the OM cavity is situated. The feedback noise can be subtracted by monitoring the actuator signal. A more optimized feedback scheme could also be implemented that injects lower noise, for example, a feedback tuned for the measured quadrature's transfer function with respect to an appropriate input quadrature that would couple minimum noise to the squeezing signal (N. Aggarwal and N. Mavalvala, in preparation).

Noise budget. The measurement is also compared to a noise budget, as shown in Fig. 3b. The total budgeted noise shown is the quadrature sum of individual contributions from the measured thermal noise, quantum noise, classical laser noises, cavity-feedback noise and differential phase noise between the signal and LO. It uses experimentally measured cavity parameters, thermal noise, BS1 and BS2 reflectivities and homodyne visibility, as listed in Table 1. The quadratures for which squeezing is obtained depend on the various OM parameters of the cavity, such as the detuning, circulating power, losses and thermal noise. We measure the cavity detuning, intracavity power and losses by measuring transfer functions from amplitude modulations on input to transmitted light (N. Aggarwal and N. Mavalvala, in preparation). The thermal noise is measured by a cross-spectrum measurement in the amplitude quadrature without the LO[33]. We have also separately calibrated all the beamsplitters, mirror reflectivities and homodyne visibility. These measured quantities are then used to predict the squeezing using a numerical model based on ref. [32]. In this model, we also include the effect of the unbalanced homodyne with an imperfect visibility and common-mode laser noises.

We then characterize the impact of technical noises by measuring their contributions. First, we measure the contribution of noise injected by the cavity-locking system. The dominant source of this noise is shot noise at PD_{lock} due to the 15% transmission of BS1. To measure this feedback noise, we measure the coherence between PD_{sqz} and the amplifier output that is fed to the phase modulator at the input. This coherence, when multiplied with the spectrum of PD_{sqz}, gives us the contribution of feedback noise. We do this at all measurement quadratures independently. We find that the impact of feedback noise is minimized at 17°, akin to other intracavity displacement noises like thermal noise.

In principle, this cavity-feedback noise could be subtracted from the final result, as it is a measured quantity, but we choose not to do so for the sake of simplicity. Instead, we choose to pick off the LO beam just after the cavity-feedback phase modulator, so that there is common-mode rejection of this locking loop phase noise at the homodyning stage at BS2. The common-mode rejection by the homodyne detection also allows us to cancel frequency noise originating from the NPRO laser, without requiring a frequency stabilization servo. Any scheme to measure squeezing not purely in the amplitude quadrature requires mixing the signal beam with an LO that is phase-coherent with it, and so one always has the ability to reject common-mode noise in this fashion. Also note that there is no risk of generating apparent squeezing after BS2 by deriving the LO from the cavity-locking field (for example, from feedback-squashing of the in-loop field), because the LO and signal fields are both out of loop[30].

Additionally, displacement fluctuations that are relative between the LO and the signal path cause an effective phase noise in the measurement. We refer to this as the differential phase noise, and we measure it by analysing the measured noise at 17°. At this quadrature, all displacement noises including the feedback noise are cancelled, and the quantum noise contribution is at the shot-noise level. We thus attribute all noise above shot noise at 17° to this relative phase noise. It may also be worth noting that the large peak in the differential phase noise near ~40 kHz is due in part to electronics noise, but mostly to the resonance of the piezo used to control the LO phase. This could be improved by re-engineering the piezo mount to have a higher resonance. We calculate the contribution of phase noise in all other quadratures by assuming that it is maximum at 90° quadrature and scaling it sinusoidally.

Finally, we are left with excess loss in the detection path. We fit this loss by adding a frequency- and quadrature-independent loss to the noise budget. We find an excess loss of $22 \pm 1\%$, which agrees with the measured loss of $21 \pm 8\%$. Note that optical loss is the only effect where a single scalar would be sufficient to explain the measurement over all quadratures and frequencies. All of the above contributions to the noise budget are shown in Extended Data Figs. 2 and 3 (as a function of measurement quadrature in Extended Data Fig. 2 and as a function of frequency in the squeezing quadrature in Extended Data Fig. 3).

Table 1 | Experimental parameters determined from measurements in the laboratory

BS1 reflectivity	85%
BS2 reflectivity	96.5%
Input coupler transmission	50 ppm
Cantilever mirror transmission	250 ppm
Cavity losses	250 ± 20 ppm
Cavity linewidth HWHM (γ)	650 kHz
Cavity detuning	0.33γ
Homodyne visibility	0.93
Intracavity power	260 ± 30 mW
Signal power $\left(\lvert t\mathbf{E}_S\rvert^2\right)$	58 ± 4 μW
LO power $\left(\lvert r\mathbf{E}_{LO}\rvert^2\right)$	$0-30 \pm 3$ μW
Detected power $\left(\lvert\mathbf{E}_{sqz}\rvert^2\right)$	49 ± 3 μW
Detection inefficiency and extra losses	$21 \pm 8\%$

See Methods for definitions.

Correlations. Consider splitting an intensity-squeezed beam onto two photodetectors. For convenience, let us split it as 50%. The amplitude quadrature of the two fields hitting the photodetectors may then be written as

$$a_1 = \frac{e^{-r}x_1 + c - y_1}{\sqrt{2}} \tag{1}$$

$$b_1 = \frac{e^{-r}x_1 + c + y_1}{\sqrt{2}} \tag{2}$$

where x_1 is the vacuum that has been squeezed by the factor e^{-r}, c represents any classical noise that might be present and y_1 is the vacuum that enters at the beamsplitter.

If we measure the the averaged cross-power spectrum of the resulting photocurrents, but do not take the absolute value, we find

$$\langle S_{ab}\rangle = \frac{1}{2}\left(e^{-2r} + S_c - 1\right)\alpha\beta \tag{3}$$

where we have normalized shot noise to 1 and assumed detector 'a' has a relative gain of α and detector 'b' has a relative gain β, and S_c is the power spectrum of the classical noise scaled to shot noise. All the cross terms between x_1, y_1 and c will average to 0, as they are uncorrelated. If the original field is squeezed, then that requires $e^{-2r} + S_c < 1$, which would then imply $\langle S_{ab}\rangle < 0$. Note that if this is not satisfied, such that we have classical noise that destroys the squeezing, then $e^{-2r} + S_c > 1$, which requires $\langle S_{ab}\rangle > 0$. Therefore, by looking at the sign of the average cross-power spectrum, one can definitively prove whether squeezing is present or not.

To interpret this, when the beam is limited by classical noise, the power fluctuations hitting both PDs are identical and positively correlated. If the beam is exactly shot-noise-limited, the power fluctuations hitting the two PDs are uncorrelated. With a perfectly amplitude-squeezed beam, the power fluctuations are exactly anticorrelated.

We may write the individual power spectra as

$$\frac{S_a}{\alpha^2} = \frac{S_b}{\beta^2} = \frac{e^{-2r} + S_c + 1}{2} \tag{4}$$

then define the normalized correlation as

$$C = \frac{\langle S_{ab}\rangle}{\sqrt{S_a S_b}} = \frac{e^{-2r} + S_c - 1}{e^{-2r} + S_c + 1} \tag{5}$$

This is convenient, because it supplies a unitless measure of the nature of the noise and is independent of the relative gain of the photodetectors. This C is similar to the square root of coherence, but retains phase information. In fact, the coherence may be written as CC^*.

We can see that if the field is entirely classical so that S_c dominates, then $C = +1$. Similarly, if the beam is exactly shot-noise-limited without squeezing, then $C = 0$. Finally, for an infinitely squeezed field with no classical noise, $C = -1$.

To simplify, let us call the total noise PSD of the original beam relative to shot noise $R = e^{-2r} + S_c$, in which case

$$C = \frac{\langle S_{ab} \rangle}{\sqrt{S_a S_b}} = \frac{R-1}{R+1} \tag{6}$$

This leads to

$$R = \frac{1+C}{1-C} \tag{7}$$

Thus, by measuring C, we have a method to measure the amount of noise relative to shot noise, independent of our ability to calibrate shot noise.

This treatment is simplified by not propagating the d.c. carriers of the fields. The final physical result becomes invariant of the beamsplitter convention if one keeps track of the d.c. carrier fields. The cross spectrum $\langle S_{ab} \rangle$ is negative for a squeezing beam x, irrespective of the beamsplitter convention, as long as the carrier of field y is smaller than the carrier of field x. This condition is trivially satisfied in our measurement, because y is coming from vacuum fluctuations, with a zero d.c. field.

To include the effects of uncorrelated electronics noise on the photodetectors, we may rewrite the power spectra for each detector as

$$S_a = \alpha^2 \frac{R+1}{2} + \alpha^2 S_{da} \tag{8}$$

$$S_b = \beta^2 \frac{R+1}{2} + \beta^2 S_{db} \tag{9}$$

where S_{da} and S_{db} are the PSDs of each detector from electronics noise. The resulting normalized correlation is

$$\begin{aligned} C &= \frac{\langle S_{ab} \rangle}{\sqrt{S_a S_b}} = \frac{R-1}{\sqrt{(R+1+S_{da})(R+1+S_{db})}} \\ &= \frac{R-1}{R+1}\left[\sqrt{1+\frac{S_{da}}{1+R}}\sqrt{1+\frac{S_{db}}{1+R}}\right]^{-1/2} \\ &= \eta \frac{R-1}{R+1} \end{aligned} \tag{10}$$

where $\eta \leq 1$ is an effective efficiency of the measurement. In our experiment, because the dark noise is far below shot noise (Extended Data Fig. 4), the efficiency η is close to 1. If instead one had a lower efficiency, we can see from equation (10) that electronics noise will make observed correlations trend towards 0, and the inferred quantum noise level to shot noise.

Tunable homodyne detector. In our experiment, we opt to use single-photodiode homodyne detection. Instead of combining the signal beam with the LO on a 50–50 beamsplitter, we combine it on a highly asymmetric beamsplitter. We measure on the output port, which transmits the larger signal fraction and reflects the smaller fraction of the LO. Although this scheme introduces some loss of signal, it works with just a single photodetector and eliminates the need for performing perfect subtraction that is needed in a balanced homodyne. Because the amount of squeezing expected in this experiment is relatively low, the reduction in squeezing due to this beamsplitter loss is small.

We show, in the following, that the signal quadrature in which the measurement is performed is given by the angle made by the resultant of vector addition of the carrier of signal and LO with respect to the signal, as displayed in Extended Data Fig. 5. Similarly, the LO quadrature measured is given by the angle this resultant makes with the LO:

$$\mathbf{E}_{sqz} = t\mathbf{E}_S + r\mathbb{R}(\theta)\ \mathbf{E}_{LO} \tag{11}$$

$$\tan\phi_S = \frac{rE_{LO}\sin\theta}{rE_{LO}\cos\theta + tE_S} \tag{12}$$

$$\tan\phi_{LO} = \frac{-tE_S\sin\theta}{rE_{LO} + tE_S\cos\theta} \tag{13}$$

$$\mathbf{E}_{sqz} = |\mathbf{E}_{sqz}|\ \mathbf{U}(\phi_S) \tag{14}$$

Here, $\mathbf{E}$ represents the strength of the carrier of signal S, LO and the resultant (sqz). Variable t is the amplitude transmitivity ($\sqrt{0.965}$) and r is the amplitude reflectivity ($\sqrt{0.035}$) of the beamsplitter. We define a unit vector $\mathbf{U}(\phi_S)$, which represents a vector in the direction of the resultant, and determines the measured quadrature. Using ref. [32], we can also calculate the loss effect of the beamsplitter. We define $\mathbf{e}$ as the fluctuations on the field, normalized such that the shot noise is $|\mathbf{E}|^2$ (N. Aggarwal and N. Mavalvala, in preparation). We then propagate these fluctuations from the signal and the LO as they interfere on the beamsplitter:

$$\mathbf{e}_{sqz} = t\mathbf{e}_S + re^{i\phi}\mathbb{R}(\theta)\ \mathbf{e}_{LO} \tag{15}$$

$$\mathbf{E}_{sqz} \cdot \mathbf{e}_{sqz} = |\mathbf{E}_{sqz}|\ \mathbf{U}(\phi_S)^\dagger\ \mathbf{e}_{sqz} \tag{16}$$

$$S_{sqz}(\phi_S) = \mathbf{U}(\phi_S)^\dagger\ \mathbf{e}_{sqz}\ \mathbf{e}_{sqz}^\dagger\ \mathbf{U}(\phi_S) \tag{17}$$

$$= \mathbf{U}(\phi_S)^\dagger \left(t^2\mathbf{e}_S\mathbf{e}_S^\dagger + r^2\mathbb{R}(\theta)\ \mathbf{e}_{LO}\mathbf{e}_{LO}^\dagger\mathbb{R}(\theta)^\dagger\right)\mathbf{U}(\phi_S) \tag{18}$$

$$= t^2 S_S(\phi_S) + r^2 \tag{19}$$

where we have assumed that the LO is shot noise limited, and defined $S_S(\phi_S) = \mathbf{U}(\phi_S)^\dagger\ \mathbf{e}_S\mathbf{e}_S^\dagger\ \mathbf{U}(\phi_S)$ as the spectral density of the signal if measured perfectly with a balanced homodyne detector at the quadrature ϕ_S. The above equations show that the total spectral density measured, $S_{sqz}(\phi_S)$ is a combination of $S_S(\phi_S)$ and 1, in the ratio of the beamsplitter's reflectivity.

Data availability

Source Data are provided with this paper. All other data that support the plots within this paper and other findings of this study are referenced under https://doi.org/10.5281/zenodo.3694290.

Code availability

All code that support the plots within this paper and other findings of this study is referenced under https://doi.org/10.5281/zenodo.3694290. It can be downloaded from GitLab at https://git.ligo.org/nancy.aggarwal/room-temperature-optomechanical-squeezing.git and from GitHub at https://github.com/nancy-aggarwal/room-temperature-optomechanical-squeezing_github.git.

References

53. Oelker, E. et al. Ultra-low phase noise squeezed vacuum source for gravitational wave detectors. *Optica* **3**, 682–685 (2016).

Acknowledgements

This work was supported by National Science Foundation grants PHY-1707840, PHY-1404245, PHY-1806634 and PHY-1150531. We are particularly grateful to V. Sudhir, L. McCuller and M.J. Yap for valuable discussions and for their detailed comments on this manuscript. The microresonator manufacturing was carried out at the UCSB Nanofabrication Facility. We also thank MathWorks for their computing support.

Author contributions

N.A. led the work, with this being the major focus of her doctoral thesis. She also conducted a theoretical study to optimize the experimental parameters being used in this experiment. J.C. and T.C. built the optomechanical cavity and the vacuum system at LSU, where the measurements were performed. J.C., N.A. and T.C. built the detection system for this measurement. T.J.C., N.A. and T.C. made the measurements and performed the data analysis. N.A. wrote the manuscript with help from T.C., T.J.C., J.C., R.L. and N.M. N.A., J.C., A.L., R.L. and T.C. designed the mechanical oscillator used in this experiment. P.H., D.F. and G.D.C. fabricated the mechanical oscillators used in this experiment. T.C. and N.M. supervised the whole project.

Competing interests

The authors declare no competing interests.

Additional information

Extended data is available for this paper at https://doi.org/10.1038/s41567-020-0877-x.

Supplementary information is available for this paper at https://doi.org/10.1038/s41567-020-0877-x.

Correspondence and requests for materials should be addressed to N.A., T.C. or N.M.

Reprints and permissions information is available at www.nature.com/reprints.

Peer review statement *Nature Physics* thanks Ryutaro Takahashi, Andre Xuereb and the other, anonymous, reviewer(s) for their contribution to the peer review of this work.

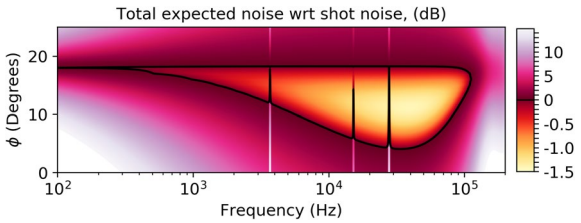

Extended Data Fig. 1 | Expected squeezing with lower detection loss and in the absence of technical noises. The differential phase noise masks the squeezing at low frequencies, whereas the noise injected by the cavity feedback electronics degrades the high frequency side of the correlations. Once these technical noises have been suppressed, and the optical losses have been lowered, we would expect to see about 1.5 dB of squeezing from this system. This limit comes from a combination of escape efficiency and thermal noise (N. Aggarwal et al., in preparation).

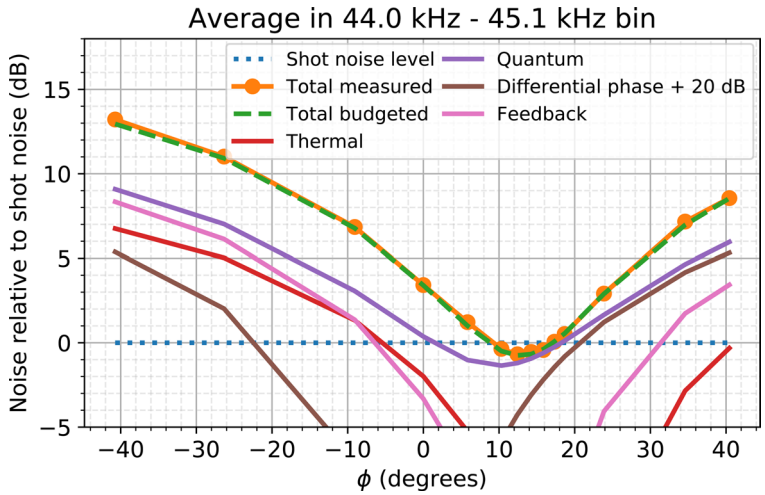

Extended Data Fig. 2 | Noise budget: contributing noise sources compared to the measurement as a function of quadrature, averaged over a 1 kHz bin. Note that a 20 dB offset has been added to the differential phase noise in order to be visible on the same axis. Measured noise is shown in orange. Also shown are the contributions from quantum noise (with excess loss) in purple, thermal noise in red, differential phase noise in brown, and cavity-feedback noise in pink. The quadrature sum of all these contributions is shown in dashed green. All noises are relative to shot noise and are shown in dBs.

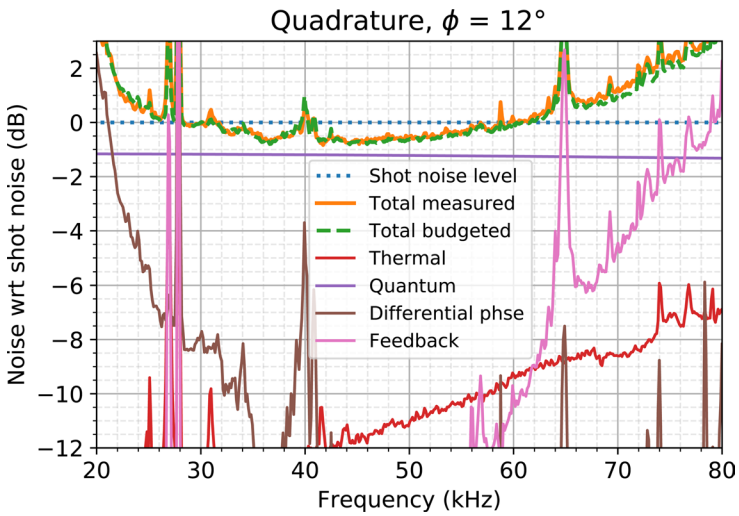

Extended Data Fig. 3 | Noise budget: contributing noise sources compared to the measurement as a function of frequency at the squeezing quadrature, 12°. Measured noise is shown in orange. Also shown are the contributions from quantum noise (with excess loss) in purple, thermal noise in red, differential phase noise in brown, and cavity-feedback noise in pink. The quadrature sum of all these contributions is shown in dashed green. All noises are relative to shot noise and are shown in dBs.

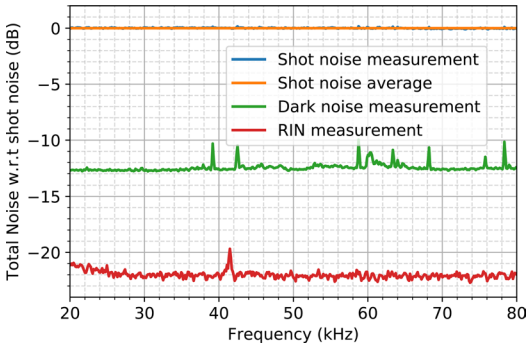

Extended Data Fig. 4 | Classical laser intensity noise and dark noise, shown relative to shot noise. Since we always keep the total detected power on PD_{sqz} constant (and just change the local oscillator (LO) power to change the measurement quadrature), the relative dark noise and classical laser intensity noise can just be scaled to that power.

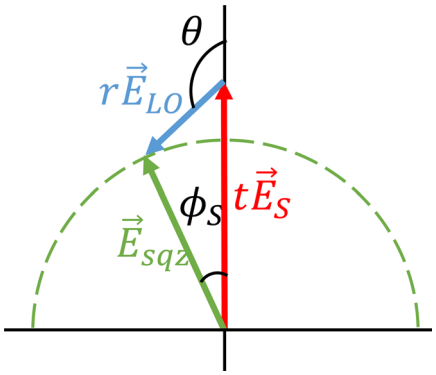

Extended Data Fig. 5 | A phasor diagram showing how the tunable homodyne detector selects the measurement quadrature. The sum of the local oscillator (LO) field (blue) and the signal field (red) selects the quadrature that is being measured (green). In the entire manuscript, we report this angle θ_s as the measurement quadrature. We determine the quadrature by knowing the power in all the three fields, and the visibility. The dashed green circle represents a contour of constant detection power. In order to keep the shot noise reference unchanged, we choose to always lock PDsqz with a constant total detected power, and vary the LO power to change the measurement quadrature. This has the effect of changing the angle θ of the LO.

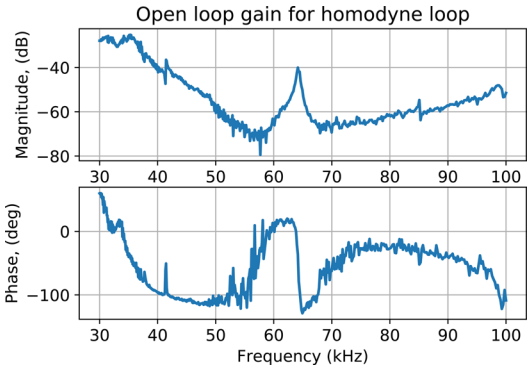

Extended Data Fig. 6 | Measurement of the open loop transfer function of the homodyne locking loop around the squeezing frequency band. Since this loop is designed only to suppress large path length fluctuations between the local oscillator and the signal at low frequencies (< 1 kHz), this loop has close to zero gain at our measurement frequencies.